INTERNATIONAL JOURNAL OF OPTIMIZATION IN CIVIL ENGINEERING
Int. J. Optim. Civil Eng., 2014; 4(4):473-490

COLLIDING BODIES OPTIMIZATION FOR DESIGN OF ARCH DAMS WITH FREQUENCY LIMITATIONS

A. Kaveh[*,†] and V.R. Mahdavi
Center of Excellence for Fundamental Studies in Structural Engineering, Iran University of Science and Technology, Narmak, Tehran-16, Iran

ABSTRACT

In this paper, optimal design of arch dams is performed under frequency limitations. Colliding Bodies Optimization (CBO), a recently developed meta-heuristic optimization method, which has been successfully applied to several structural problems, is revised and utilized for finding the best feasible shape of arch dams. The formulation of CBO is derived from one-dimensional collisions between bodies, where each agent solution is considered as the massed object or body. The design procedure aims to obtain minimum weight of arch dams subjected to natural frequencies, stability and geometrical limitations. Two arch dam examples from the literature are examined to verify the suitability of the design procedure and to demonstrate the effectiveness and robustness of the CBO in creating optimal design for arch dams. The results of the examples show that CBO is a powerful method for optimal design of arch dams.

Received: 14 July 2014; Accepted: 20 November 2014

KEY WORDS: colliding bodies optimization; arch dam; optimal design; frequency constraints.

1. INTRODUCTION

An arch dam can be defined as a concrete structure, the base of which is less than half of its height and for transmission of part of the water load laterally into the valley flanks has to rely on its curvature in the plan. Arch dams may contain as little as 20% of the concrete of the equivalent gravity dams. Arch dams are designed, both in the single or double-curvature

---

[*]Corresponding author: Center of Excellence for Fundamental Studies in Structural Engineering, Iran University of Science and Technology, Narmak, Tehran-16, Iran
[†]E-mail address: alikaveh@iust.ac.ir (A. Kaveh)

forms. In double-curvature form, for minimizing the volume of an arch dam; its radius of curvature should change from crest to base [1].

Natural frequencies are fundamental parameters affecting the dynamic behavior of the structures. Therefore, some limitations should be imposed on the natural frequency range to reduce the domain of vibration and also to prevent the resonance phenomenon in dynamic response of Optimization of structures based on frequency limitation has been widely employed during the last two decades. Mass reduction conflicts with the frequency constraints, especially when they are lower bounded. Therefore, frequency constraints are highly non-linear, non-convex and implicit with respect to the design variables [2]. To implement a practical arch dam design, many constraints such as stress, displacement, stability requirement, and frequency constraints should be considered [1]. In the present study, for simplicity of the optimization operations and comparison with the existing results from literature, only frequency and some geometrical constraints are considered.

Recently some progress has been made in optimum design of arch dams considering different constraints. Almost all of these have used conventional methods for analysis approximation and optimization. These methods usually employ derivative calculations and can be trapped in local optima. The shape optimization of arch dams has been developed after appearing and development of finite element method in late 1950's. Rajan [3], Mohr [4] and Sharma [5] developed solutions based on membrane shell theory. Sharpe [6] was the first to formulate the optimization as a mathematical programming problem. A similar method was also adopted by Rickeetts and Zienkiewicz [7] who used finite element method for stress analysis and Sequential Linear Programming (SLP) for the shape optimization of arch dams under static loading.

Recently, the Colliding Bodies Optimization (CBO) has been introduced by authors as an efficient optimization algorithm for the optimum design of structures. The CBO algorithm is based on laws of collision between bodies. This algorithm can be considered as a multi-agent approach, where each agent is a Colliding Body (CB). As will be explained in detail, each CB is considered as a massed object with a specified the mass and velocity before the collision. After occur of collision, each CB moves to the new position according to the new velocity [8-10]. In this study, the CBO algorithm is employed for volume or cost optimization of arch dams, considering the concrete volume and the casting areas. The results of the solved examples demonstrate that CBO leads to better results than CSS and PSO (see Kaveh [11] for recently developed meta-heuristic algorithms).

2. GEOMETRICAL MODEL OF ARCH DAM

2.1 Shape of the central vertical section

The shape of a double-curvature arch dam has two basic characteristics: curvature and thickness. Both the curvature and the thickness change in horizontal and vertical directions. For the central vertical section of double-curvature arch dam, as shown in Fig. 1, one polynomial of nth order is used to determine the curve of upstream boundary and another polynomial is employed to determine the thickness. In this study, a parabolic function is considered for the curve of upstream face as:

$$y(z) = b(z) = -sz + \frac{sz^2}{2\beta h} \tag{1}$$

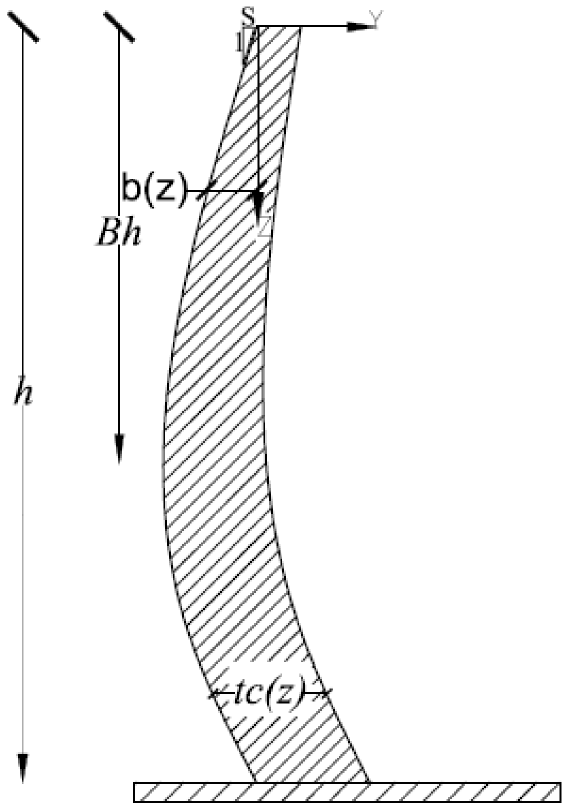

Figure 1. Central vertical section of an arch dam

where h and s are the height of the dam and the slope at crest respectively, and the point where the slope of the upstream face equals to zero is $z=\beta$ h in which β is constant.

By dividing the height of dam into n equal segments containing n + 1 levels, the thickness of the central vertical section can be expressed as:

$$t_c(z) = \sum_{i=1}^{n+1} L_i(z) t_{ci} \tag{2}$$

in which t_{ci} is the thickness of the central vertical section at the ith level. Also, in the above relation $L_i(z)$ is a Lagrange interpolation function associated with the ith level and can be defined as:

$$L_i(z) = \frac{\prod_{K=1}^{n+1}(Z - Z_K)}{\prod_{K=1}^{n+1}(Z_i - Z_K)} \qquad i \neq k \tag{3}$$

where z_i denotes the z coordinate of the ith level in the central vertical section.

3.2 Shape of the horizontal section

As shown in Fig. 2, for the purpose of symmetrical canyon and arch thickening from crown to abutment, the shape of the horizontal section of a parabolic arch dam is determined by the following two parabolas:

At the upstream face of the dam:

$$y_u(x,z) = \frac{1}{2r_u(z)}x^2 + b(z) \tag{4}$$

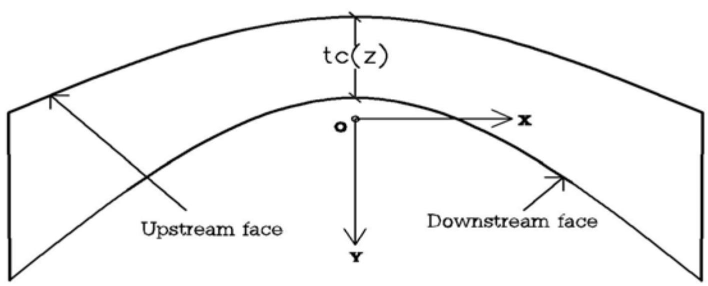

Figure 2. The parabolic shape of a horizontal section of dam

At the downstream face of the dam:

$$y_d(x,z) = \frac{1}{2r_d(z)}x^2 + b(z) + t_c(z) \tag{5}$$

where r_u and r_d are radii of curvatures corresponding to the upstream and downstream curves, respectively. Here, functions of nth order with respect to z can be used for these radii:

$$r_u = \sum_{i=1}^{n} L_i r_{ui}$$
$$r_d = \sum_{i=1}^{n} L_i r_{di} \tag{6}$$

where r_{ui} and r_{di} are the values of r_u and r_d at the ith level, respectively.

3. ARCH DAM OPTIMIZATION PROBLEMS

The optimization problem can formally be stated as follows:

$$\begin{array}{ll} \text{Find} & X = [x_1, x_2, x_3, .., x_n] \\ \text{to minimizes} & Mer(X) = f(X) \times f_{penalty}(X) \\ \text{subjected to} & g_i(X) \leq 0,\ i = 1,2,\ldots,m \\ & x_{imin} \leq x_i \leq x_{imax} \end{array} \tag{7}$$

where X is the vector of design variables with n unknowns, g_i is the ith constraint from m inequality constraints and $Mer(X)$ is the merit function; $f(X)$ is the cost ; $f_{penalty}(X)$ is the penalty function which results from the violations of the constraints corresponding to the response of the arch dam. Also, x_{imin} and x_{imax} are the lower and upper bounds of design variable vector, respectively.

Exterior penalty function method is employed to transform the constrained dam optimization problem into an unconstrained one as follows:

$$f_{penalty}(X) = 1 + \gamma_p \sum_{i=1}^{m} \max(0, g_j(x)) \tag{8}$$

where γ_p is penalty multiplier.

3.1 Design variables

The most effective parameters for creating the arch dam geometry were mentioned in Section 2. The parameters can be adopted as design variables:

$$X = \{ s \quad \beta \quad t_{c1} \quad .... \quad t_{cn} \quad r_{u1} \quad .... \quad r_{un} \quad r_{d1} \quad .... \quad r_{dn} \} \tag{9}$$

Where X vector of design variables contains $3n$+2 shape parameters of arch dam.

3.2 Design constraints

Design constraints are divided into some groups including the behavioral, geometrical and stability constraints. The behavioral constraints are the restricted natural frequencies that are defined as follows:

$$frl_n \leq fr_n \leq fru_n \Rightarrow \begin{cases} 1 - \dfrac{fr_n}{frl_n} \leq 0 \\ \dfrac{fr_n}{fru_n} - 1 \leq 0 \end{cases}, \quad n = 1,2,..., n_{fr} \tag{10}$$

where fr_n , frl_n and fru_n are the nth natural frequency, lower bound and upper bound of the *n*th natural frequency, respectively. Here, *nfr* is the number of natural frequencies. The most important geometrical constrains are those that prevent from intersection of upstream face and downstream face as:

$$r_{dn} \le r_{un} \Rightarrow \frac{r_{dn}}{r_{un}} - 1 \le 0, \quad n = 1,2,3 \tag{11}$$

where r_{dn} and r_{un} are the radii of curvatures at the down and upstream faces of the dam in *n*th position in *z* direction. The geometrical constrain that is applied to facilities the construction, is defined as:

$$s \le s_{all} \Rightarrow \frac{s}{s_{all}} - 1 \le 0 \tag{12}$$

Where s is the slope of overhang at the downstream and upstream faces of dam and s_{all} is its allowable value.

3.3 Cost function

The cost function is the construction cost of the dam, which may be expressed as:

$$f(X) = p_v v(X) + p_a a(X) \tag{13}$$

Where *v*(X) and *a*(*X*) are the concrete volume and the casting area of dam body. *pv* and *pa* are the unit price of concrete and casting, respectively.

The volume of concrete can be determined by integrating from dam surfaces as:

$$v(X) = \iint_{Area} \left| y_d(x,z) - y_u(x,z) \right| dxdz \tag{14}$$

In which *Area* is an area produced by projecting of dam on *xz* plane. The areas of casting can be approximately calculated by summing of the areas of upstream and downstream faces as follows:

$$a(X) = a_u(X) + a_d(X) = \iint_{Area} \sqrt{1 + (\frac{dy_u}{dx})^2 + (\frac{dy_u}{dz})^2}\, dxdz + \iint_{Area} \sqrt{1 + (\frac{dy_d}{dx})^2 + (\frac{dy_d}{dz})^2}\, dxdz \tag{15}$$

Where a_u and a_d are the casting areas of upstream and downstream faces, respectively. To evaluate *v*(*X*) and *a*(*X*) a computer program is coded using MATLAB [12].

3.4 Water-dam interaction

In this study, the generalized Westergaard [13] method is used in order to include dam-reservoir interaction. In this method, hydrodynamic pressure exerted on the face of the dam is equivalent to the inertia forces of a body of water attached to the dam and moving back and forth with the dam while the rest of reservoir water remains inactive [14]. The general formulation is based on the parabolic shape for body of water with a base width equal to 7/8 of the height, as shown in Fig. 3. Finally, a full 3x3 added-mass matrix at each nodal point on the upstream face of the dam is obtained as:

$$m_{\alpha} = \alpha A \lambda^{T} \lambda \tag{16}$$

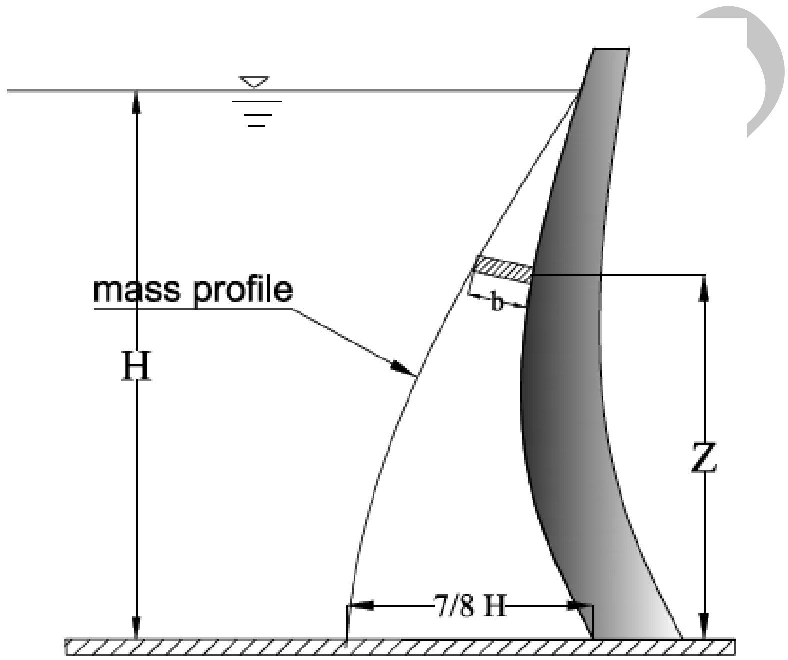

Figure 3. The generalized Westergaard added mass method

Which *A* is the tributary surface area and λ^{T} is a vector of normal direction cosines for each point. A is the Westergaard pressure coefficient:

$$\alpha = \rho_{w} b = \frac{7}{8} \rho_{w} \sqrt{H(H-Z)} \tag{17}$$

Which ρ_w is the density of water, H and Z are as defined in Fig. 3.

In the analysis, the dam-foundation interaction is also omitted to avoid the extra complexities that would otherwise arise.

3.5 Verification of the finite element models

In order to validate the finite element model with the considered assumptions, an idealized model of Morrow Point arch dam (Fig. 4) which is located 263 km southwest of Denver, Colorado, is investigated. The properties of the dam in details can be found in [15]. The physical and mechanical properties involved here are the concrete density (2483N.s^2/m^4), the concrete poison's ratio (0.2) and the concrete elasticity (27580×10^4 MPa).

In the present work the first two natural frequencies of the mode of Morrow Point dam are determined from the frequency response function for the crest displacement and the results are compared to those reported in the literature [15]. The natural frequencies from the other literatures and present work are given in Table 1. It can be observed that a good conformity is achieved between the results of present work with those of the previously reported results.

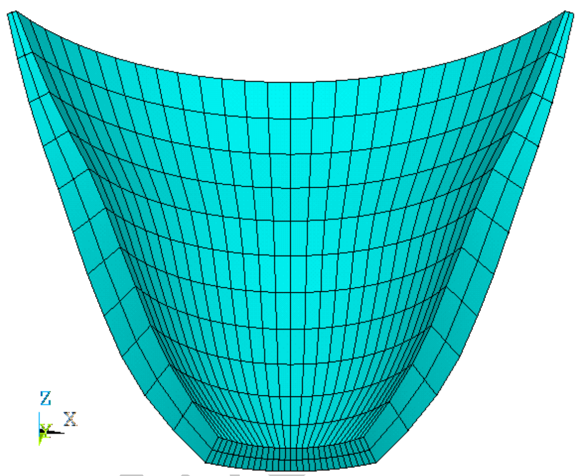

Figure 4. The finite element model of the Morrow Point arch dam

Table 1: Natural frequencies (Hz) of the Morrow Point arch dam

Case	Reservoir	Natural frequencies (Hz)			
		Tan & Chopra (Tan Chopra 1996)		Present work	
		Symmetric mode	Antisymmetric mode	Symmetric mode	Antisymmetric mode
1	Empty	4.27	3.81	4.30	3.77
2	Full	2.82	2.91	2.84	3.05

4. THE CBO ALGORITHM

The CBO mimic the one-dimensional collision law between bodies (Fig. 5). In the CBO, each solution candidate X_i containing a number of variables (i.e. $X_i = \{X_{i,j}\}$) is considered as a colliding body (CB) with mass *m*. The magnitude of mass of each CB is proportional to this fitness. The massed objects composed of two main groups equally; namely stationary and moving objects. In order to improve the positions of the moving objects and to push stationary objects towards better positions, the moving objects moves to follow stationary objects and a collision occur between pairs of objects. After the collision, new positions of the colliding bodies are updated based on the new velocity by using the collision laws; and the lighter and heavier CB moves sharply and slowly, respectively.

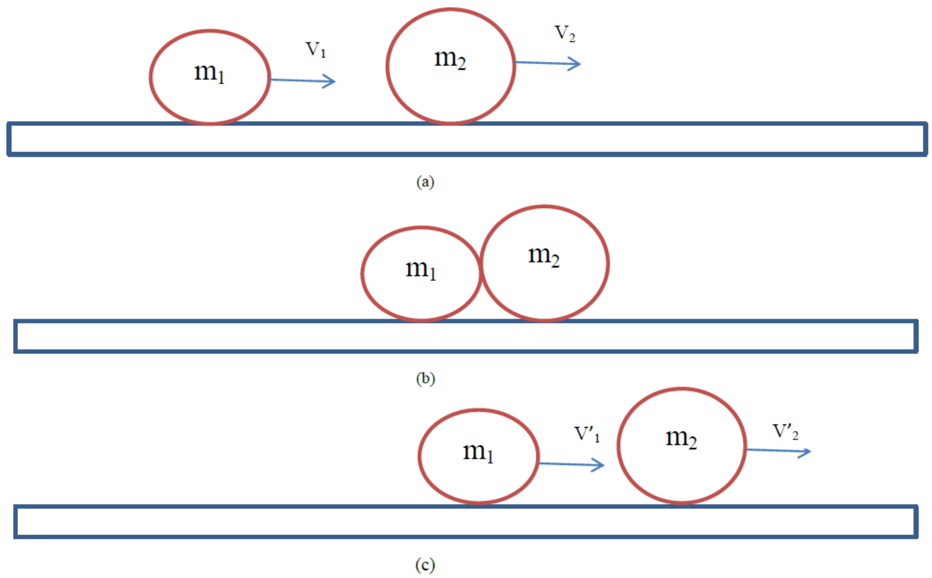

Figure 5. The collision between two bodies, (a) before collision, (b) colliding, (c) after collision

The pseudo-code for the CSS algorithm can be summarized as follows:

Step 1: *Initialization*. The initial positions of CBs are determined with random initialization of a population of individuals in the search space:

$$x_i^0 = x_{\min} + rand(x_{\max} - x_{\min}), \quad i = 1,2,\ldots,n, \tag{18}$$

Where, x_i^0 determines the initial value vector of the i th CB. $x_{\min}$ and $x_{\max}$ are the minimum and the maximum allowable values vector for the variables; *rand* is a random number in the interval [0,1]; and n is the number of CBs.

Step 2: *Mass determination*. Calculate the body mass for each CB as:

$$m_k = \frac{1}{fit(k)}, \quad k = 1,2,\ldots,n \tag{19}$$

Where *fit(i)* represents the fitness value of the agent i; n is the number of population size. It can be seems that a CB with good values exerts a larger mass than the bad ones.

Step 3: *Mating of bodies*. The CBs fitness is sorted in an ascending order (Fig. 6a). The sorted CBs are divided to two groups equally; stationary and moving group. In stationary group, the CBs are good agents which these are stationary, and the velocity of these bodies before collision is zero:

$$v_i = 0, \quad i = 1, \ldots, \frac{n}{2} \tag{20}$$

In moving group, the CBs move toward the stationary CBs. Then better and worse CBs, i.e. agents with upper fitness value, of each group are collided together (Fig. 6b). The change of the body position represents the velocity of these bodies before collision as:

$$v_i = x_{i-\frac{n}{2}} - x_i, \qquad i = \frac{n}{2} + 1, \ldots, n \tag{21}$$

Where, v_i and x_i are the velocity and position vector of the i th CB in this group, respectively; $x_{i-\frac{n}{2}}$ is the i th CB pair position of x_i in the previous group.

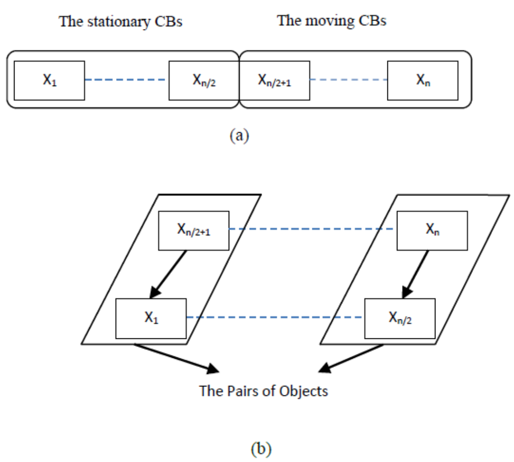

Figure 6. (a) The sorted CBs in an increasing order, (b) The pairs of objects for the collision

Step 4: *Updating velocities.* After the collision, the velocity of the bodies in each group are evaluated using collision laws and the velocity before collision. The velocity of each moving CBs after the collision is:

$$v_i' = \frac{(m_i - \varepsilon m_{i-\frac{n}{2}}) v_i}{m_i + m_{i-\frac{n}{2}}}, \quad i = \frac{n}{2} + 1, \ldots, n \tag{22}$$

Where, v_i and v_i' are the velocity of the i th moving CB before and after the collision, respectively; m_i is the mass of the i th CB; $m_{i-\frac{n}{2}}$ is mass of the i th CB pair. The velocity of each stationary CB after the collision is:

$$v_i^{'} = \frac{(m_{i+\frac{n}{2}} + \varepsilon m_{i+\frac{n}{2}})v_{i+\frac{n}{2}}}{m_i + m_{i+\frac{n}{2}}}, \quad i = 1,...,\frac{n}{2} \tag{23}$$

Where, $v_{i+\frac{n}{2}}$ and $v_i^{'}$ are the velocity of the i th moving CB pair before and the i th stationary CB after the collision, respectively; m_i is mass of the i th CB; $m_{i+\frac{n}{2}}$ is mass of the i th moving CB pair; ε is the coefficient of restitution (COR), which is defined as the ratio of the separation velocity of two agents after collision to the approach velocity of two agents before collision. For most of the real objects, ε is between 0 and 1, which after collision the separation velocity of bodies is low and high, respectively. Therefore, to control exploration and exploitation rate, COR decreases linearly from unity to zero and ε is defined as:

$$\varepsilon = 1 - \frac{iter}{iter_{\max}} \tag{24}$$

where *iter* is the actual iteration number and $iter_{max}$ is the maximum number of iterations.

Step 5*: Updating positions*. New positions of CBs are evaluated using the generated velocities after the collision in position of stationary CBs.

The new positions of each moving CBs is:

$$x_i^{new} = x_{i-\frac{n}{2}} + rand.v_i^{'}, \quad i = \frac{n}{2}+1,...,n \tag{25}$$

Where, x_i^{new} and $v_i^{'}$ are the new position and the velocity after the collision of the i th moving CB, respectively; $x_{i-\frac{n}{2}}$ is the old position of i th stationary CB pair. Also, the new positions of each stationary CBs is:

$$x_i^{new} = x_i + rand.v_i^{'}, \quad i = 1,...,\frac{n}{2} \tag{26}$$

Where, x_i^{new}, x_i and $v_i^{'}$ are the new position, old position and the velocity after the collision of the i th stationary CB, respectively. *rand* is a random vector uniformly distributed in the range (-1,1).

Step 6*: Terminating criterion*. The optimization is repeated from step 2 until a termination criterion, such as the maximum number of iterations, is satisfied.

Apart from the efficiency of the CBO algorithm, which is illustrated in the next section through numerical examples, the independence of the algorithm from internal parameters is one of the main advantageous of the CBO algorithm. Also, the formulation of CBO algorithm does not use the memory which saves the best-so-far solution (i.e. the best position of agents from the previous iterations).

5. NUMERICAL EXAMPLES

In this section, two common arch dam are optimized utilizing the new algorithm. A finite element model based on free vibration analysis for the double-curvature arch dam is presented. The arch dam is treated as a three dimensional linear structure. To mesh of the arch dam body eighty-node isoperimetric solid element is used. To evaluate the eigenvalues of arch dam a computer program is coded using Opensees [16].

5.1 Hypothetical model

As the first example, a well-known benchmark problem in the field of shape optimization of the arch dam, a dam with a height of 180 m is considered. The width of the valley in its bottom and top are 40 m and 220 m, respectively (Fig. 7). For this test example, the construction cost is the objective function. The unit prices for concrete and casting are considered as pv = \$33.34 and pt = \$6.67, respectively. Material properties are: elastic modulus of E=21 GPa, poison's ratio of 0.2 and mass density of ρ=2400 kg/m^3. In this example, CBO population size is set as 20 individuals. The maximum number of iterations is also considered as 200.

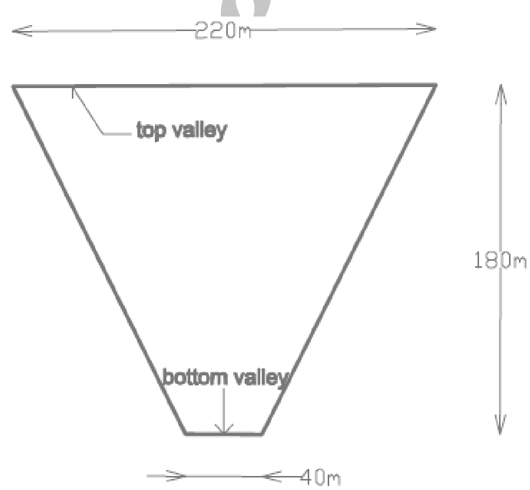

Figure 7. The valley dimensions of the arch dam

The dam is modeled by 11 shape design variables as:

$$X = \{S \quad \beta \qquad t_{c1} \quad t_{c2} \quad t_{c3} \qquad r_{u1} \quad r_{u2} \quad r_{u3} \qquad r_{d1} \quad r_{d2} \quad r_{d3} \quad \} \tag{25}$$

The lower and upper bounds of design variables using empirical design methods are considered as Varshney [17]:

$$\begin{array}{cccc} 0 \le s \le 0.3 & 4 \le t_{c1} \le 12 & 50 \le r_{u1} \le 180 & 50 \le r_{d1} \le 180 \\ 0 \le \beta \le 1 & 8 \le t_{c2} \le 30 & 40 \le r_{u2} \le 120 & 40 \le r_{d2} \le 120 \\ & 12 \le t_{c3} \le 40 & 10 \le r_{u3} \le 50 & 10 \le r_{d3} \le 50 \end{array} \tag{26}$$

In current study, the following natural frequency constraints are imposed:

$$fr_1 \ge 3Hz \quad fr_2 \ge 6.3Hz \quad fr_3 \ge 7.3Hz \quad fr_4 \ge 8.3Hz \tag{27}$$

Two cases are considered for this example:

Case 1: the reservoir is empty.

Case 2: the reservoir is full and dam-reservoir interaction is considered in the process of analysis.

This example was solved by Kaveh and Mahdavi [18] using the CSS and PSO algorithms for Case 1. Table 2 compares the optimized design and the required number of structural analyses with literature for both cases. It can be seen that the CBO algorithm finds the best design and requires less structural analyses than other optimization techniques. The optimum weight of dam is also considerably heavier for Case 2, when dam-reservoir interaction is considered. Fig. 8 shows the convergence curves of the CBO, CSS and PSO for Case 1. Although CSS and PSO were considerably faster in the early optimization iterations, CBO converged to a significantly better design without being trapped in local optima. Table 3 shows the nature frequencies of the optimized structure obtained previously by the authors and the results obtained by the present work.

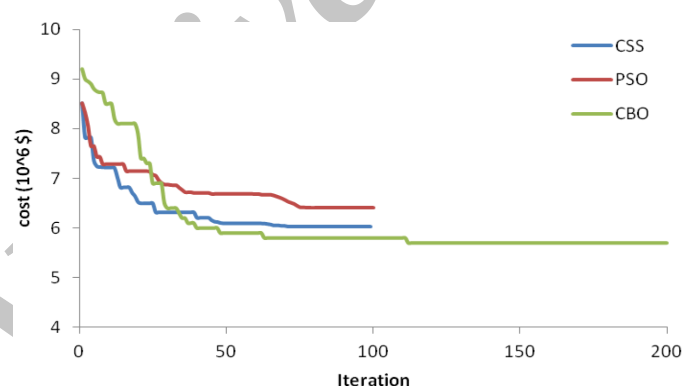

Figure 8. The convergence curves for the PSO, CSS and CBO (Case 1)

5.2 Morrow Point Arch Dam

In second example, the optimization of Morrow Point arch dam, for which the properties are mentioned previously, is examined. For this test example, volume of the concrete is the objective function. To create the dam geometry, three fifth-order functions are considered for tc(z), ru(z), and rd (z). Thus, by accounting for two shape parameters needed to define the curve of upstream face b(z), the dam can be modeled by 20 shape design variables as:

$$X = \{s \quad \beta \quad t_{c1} \quad t_{c2} \quad t_{c3} \quad t_{c4} \quad t_{c5} \quad t_{c6} \quad r_{u1} \quad r_{u2} \quad r_{u3} \quad r_{u4} \quad r_{u5} \quad r_{u6} \quad r_{d1} \quad r_{d2} \quad r_{d3} \quad r_{d4} \quad r_{d5} \quad r_{d6}\} \tag{28}$$

Table 2: Optimum designs of the arch dam obtained by different methods

Variable No.	Kaveh and Mahdavi (Kaveh and Mahdavi 2011)		Present work	
	PSO	CSS	CBO	
	Case 1		Case 1	Case 2
1	0.2577	0.0216	0.2673	0.2717
2	0.8195	0.6141	0.655	0.6876
3	8.7656	8.0144	6.6061	4.0974
4	8.9711	8.0010	8.0205	26.0802
5	17.6736	17.2981	14.5962	12.1907
6	117.6666	159.6764	171.9731	114.9598
7	79.1041	91.8348	70.1358	98.9373
8	42.8860	46.7626	30.4945	48.4383
9	63.7034	85.2251	83.1802	114.904
10	54.0178	52.3796	49.9592	47.3008
11	26.3438	29.8441	27.0186	22.9041
cost of arch dam ($\$10^6$)	6.403	6.030	5.680	9.370
number of analyses	5,000	5,000	4,000	4,000

Table 3: Natural frequencies (Hz) of the optimized arch dam

Frequency number	Kaveh and Mahdavi (Kaveh and Mahdavi 2011)		Present work	
	PSO	CSS	CBO	
	Case 1		Case 1	Case 2
1	5.056	4.492	4.668	4.285
2	6.568	6.362	6.492	6.304
3	7.375	7.300	7.300	7.742
4	8.415	8.350	8.300	8.542

The lower and upper bounds of design variables required for the optimization process can be determined using preliminary design methods [17]:

$$\begin{array}{llll} 0 \le s \le 0.3 & 3 \le t_{c1} \le 10 & 100 \le r_{u1} \le 135 & 100 \le r_{d1} \le 135 \\ 0.5 \le \beta \le 1 & 5 \le t_{c2} \le 15 & 85 \le r_{u2} \le 115 & 85 \le r_{d1} \le 115 \\ & 10 \le t_{c3} \le 20 & 70 \le r_{u3} \le 100 & 70 \le r_{d1} \le 100 \\ & 15 \le t_{c4} \le 25 & 60 \le r_{u4} \le 80 & 60 \le r_{d4} \le 80 \\ & 20 \le t_{c5} \le 30 & 45 \le r_{u5} \le 60 & 45 \le r_{d5} \le 60 \\ & 25 \le t_{c6} \le 35 & 30 \le r_{u6} \le 45 & 30 \le r_{d6} \le 45 \end{array} \tag{29}$$

Natural frequency constraints are considered as:

$$fr_1 \geq 4Hz \quad fr_2 \geq 6Hz \quad fr_4 \geq 6.8Hz \quad fr_5 \geq 9Hz \tag{30}$$

Two cases are considered for this example:

Case 1: The reservoir is empty. In order to show the effect of the number of agent on results, the agent size was set to: 10, 20, 30 and 40 individuals for this case.

Case 2: Dam-reservoir interaction is considered in the process of analysis. Similarity, to show the effect of the water depth of reservoir, the water depth is considered as 25, 50, 75 and 100 percent of the reservoir height for this case.

The maximum number of iterations is considered as 200 for both cases. Table 4 represents the design vectors and the volume of arch dam obtained utilizing various numbers of agents using the CBO algorithm. Undoubtedly, the optimum weight becomes less, if higher number of agents is considered. On other hand, the number of objective function evaluation grows in the optimization process. As it can be seen after the number of agents becomes 20, the optimum weight does not change considerably and the objective function evaluation increases. Therefore, the number of agents is considered 20 in Case 2. Table 5 lists the designs developed by the CBO algorithm for various values of water depth of reservoir. The results show that the optimum weight of arch dams is 40.28%, 34.55%, 13.56%, and 1.63% heavier than the empty reservoir (Case 1) for different water depth of 25, 50, 75 and 100 percent of the reservoir height, respectively.

Table 4: Optimum designs of the arch dam obtained by different agent sizes using the CBO algorithm for Case 1

Variable No.	Number of agents			
	10	20	30	40
S	0.1174	0.0919	0.2426	0.118
β	0.7647	0.6381	0.9049	0.6047
t_{c1}	4.806	3.0582	3.0261	3.077
t_{c2}	7.5395	5.0054	5.3826	5.0341
t_{c3}	10.1154	10.0057	10.1436	10.0029
t_{c4}	15.0472	15.0091	15.0922	15.0159
t_{c5}	20.5051	21.2606	20.0265	20.0529
t_{c6}	25.5795	29.3904	25.0384	25.6688
r_{u1}	129.393	103.5044	132.509	122.0125
r_{u2}	102.4197	101.6245	108.0625	101.541
r_{u3}	86.2968	90.0168	83.1949	81.9052
r_{u4}	67.2429	69.4739	72.2955	71.0237
r_{u5}	54.0329	47.9893	56.9688	53.1161
r_{u6}	43.0487	40.8733	40.7917	39.2411

r_{d1}	124.0519	103.4444	130.7955	115.2456
r_{d2}	100.7791	101.6211	106.4657	100.6899
r_{d3}	86.283	89.5847	82.0417	81.2649
r_{d4}	67.1989	63.532	71.9666	70.9051
r_{d5}	53.7997	47.9098	56.6816	52.9816
r_{d6}	40.197	35.3833	37.7116	38.7547
concrete volume (m^3) (10^5)	**2.2332**	**2.0958**	**2.049**	**2.0269**

Table 5: Optimum design of the arch dam obtained by different water depths using the CBO algorithm for Case 2

Variable No.	Water depths (% the reservoir height)			
	100	75	50	25
S	0.2226	0.2862	0.2771	0.273
β	0.9364	0.8427	0.5771	0.7687
t_{c1}	3.2143	3.0093	3.0045	3.0896
t_{c2}	14.6602	12.3889	7.6267	5.0814
t_{c3}	17.2727	16.4187	10.2203	10.0435
t_{c4}	15.0077	15.0161	15.2465	15.072
t_{c5}	22.3368	21.8639	23.7625	20.0689
t_{c6}	25.59	31.8375	30.7036	26.1521
r_{u1}	130.0986	117.2926	105.4596	117.4806
r_{u2}	87.53	97.9331	101.0327	106.3058
r_{u3}	96.5577	95.2853	85.4975	84.8487
r_{u4}	61.3002	73.6625	71.5594	73.878
r_{u5}	51.932	51.8508	54.9586	54.305
r_{u6}	42.8655	39.5182	41.2766	40.1442
r_{d1}	129.5493	117.0644	105.3674	107.2574
r_{d2}	86.4328	95.8001	100.8296	106.0684
r_{d3}	80.5763	77.7262	77.243	84.3591
r_{d4}	60.574	73.6579	71.3418	73.7493
r_{d5}	48.9599	51.8035	52.5522	49.7874
r_{d6}	37.2583	39.3527	35.8985	37.5047
concrete volume (m^3) (10^5)	**2.940**	**2.820**	**2.380**	**2.130**

Fig. 9 shows the convergence curves by various numbers of agents for the optimum design of arch dam using the CBO algorithm. As it can be seen, the objective function and convergence rate is decreased by increasing the number of agents.

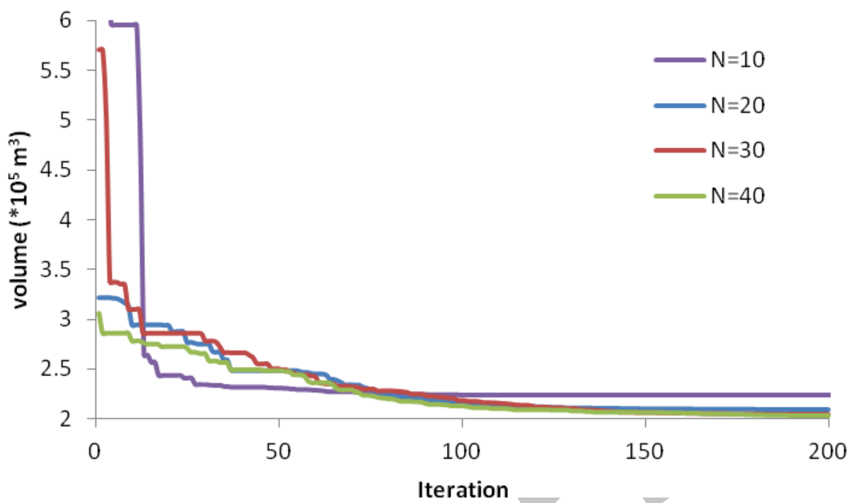

Figure 9. The convergence curves for the CBO by different number of agents (N)

6. CONCLUDING REMARKS

In this paper, a new, simple and efficient meta-heuristic algorithm, so called the Colliding Bodies Optimization (CBO), has been proposed for optimum design of arch dams. The governing laws from the physics initiate the base of the CBO algorithm, where these laws determine the movement process of the objects. In this algorithm, each agent solution considered as the colliding body (CB). After a collision of two moving body which has specified the mass and velocity, these separated with new velocity. The main advantage of the CBO is that unlike many other meta-heuristics it is parameter independent.

The shape optimization of two double-curvature arch dam is performed with frequency limitations. The concrete volume and cost of the arch dams, which includes the concrete volume and the casting areas, are considered as the objective function, with frequency, geometrical and stability constraints. Different scenarios for the water depth and the number of agents are also considered for the second example. Form the results of this study it can be seen that the CBO leads to better results than both standard CSS and PSO. Future research will investigate optimization of arch dam with different constraints and more precisely design such as, for example, stress limitation, earthquake loading and dam-foundation-water interaction.

REFERENCES

1. Sutherland J, Humm D, Chrimes M. *Historic Concrete: Background to Appraisal*, Thomas Telford Publishing, 2001.
2. Kaveh A, Zolghadr A. Truss optimization with natural frequency constraints using a hybridized CSS-BBBC algorithm with trap recognition capability, *Comput Struct* 2012; **102-103**: 14-27.
3. Rajan MKS. Shell Theory Approach for Optimization of Arch Dam Shapes, Ph.D Thesis, University of California, Berkeley, 1968.
4. Mohr GA. Design of shell shape using finite elements, *Comput Struct* 1979; **10**(5): 745-9.
5. Sharma RL. Optimal Configuration of Arch Dams, Ph.D. thesis, Indian Institute of Technology, Kanpur, 1983.
6. Sharpe R. *The Optimum Design of Arch Dams*, Institution of Civil Engineers, 1969.
7. Ricketts RE, Zienkiewicz OC. *Shape Optimization of Concrete Dams, Criteria and Assumptions for Numerical Analysis of Dams*, Quadrant Press, Swansea, London, UK, 1975.
8. Kaveh A, Mahdavai VR. Colliding bodies optimization: A novel meta-heuristic method, *Comput Struct* 2014; **139**: 18-27.
9. Kaveh A, Mahdavai VR. Colliding bodies optimization for truss optimization with multiple frequency cobstraints, *J Comput Civil Eng, ASCE* 2014, In press.
10. Kaveh A, Mahdavai VR. Colliding bodies optimization method for optimum design of truss structures with continuous variables, *Adv Eng Softw* 2014; **70**: 1-12.
11. Kaveh A. *Advances in Metaheuristic Algorithms for Optimal Design of Structures*, Springer International Publishing, Switzerland.
12. The Language of Technical Computing, MATLAB, Math Works Inc, 2009.
13. Westergaard HM. Water pressure on dams during earthquakes, *Trans Amer Soc Civil Eng* 1933; **98**: 418-33.
14. Chakrabarti A, Nalini VN. Hydrodynamic pressure on a dam with a periodically corrugated reservoir bed, *Acta Mech* 1986; **60**(1-2): 91-7.
15. Tan H, Chopra AK. Dam-foundation rock interaction effects in earthquake response of arch dams, *J Struct Eng* 1996; **122**: 528-38.
16. McKenna F, Fenves GL, Scott MH. *Open System for Earthquake Engineering Simulation,* Pacific Earthquake Engineering Research Center, University of California, Berkeley, CA, 2003.
17. Varshney RS. *Concrete Dams*, Second ed, Oxford and IBH Publishing Co, New Delhi, India, 1982.
18. Kaveh A, Mahdavai VR. Optimal design of arch dams for frequency limitations using charged system search and particle swarm optimization, *Int J Optim Civil Eng* 2011; **4**: 543-55.